

## Development of body formulations using colemanite waste in porcelain tile production

Nezahat Ediz<sup>a,\*</sup> and Arife Yurdakul<sup>b</sup>

<sup>a</sup>Dumlupınar University, Department of Ceramic Engineering, Kütahya, Turkey.

<sup>b</sup>Bruno Seramik, R&D Department, Eskişehir, Turkey

Porcelain tiles have become one of the most important products of the ceramic industry in the last decade mainly owing to their attractive physical and mechanical properties including high strength, high fracture toughness and density, excellent chemical resistance and low water absorption. The attractiveness of using porcelain has initiated intensive research work for alternative raw materials because of the depletion and the high cost of the usual materials currently used in the ceramic industry. In this research, the aim was to use boron-bearing solid wastes ( $\text{Ca}_2\text{B}_6\text{O}_{11}\cdot 5\text{H}_2\text{O}$ ) as an alternative fluxing agent to Na-feldspar ( $\text{NaAlSi}_3\text{O}_8$ ) in fast-fired porcelain tile bodies produced under industrial conditions without altering the microstructural, physical and chemical properties required from the final product. For this purpose, the suitability of the colemanite-added porcelain tile bodies to fast-firing conditions was determined using an optical dilatometer. It was then understood that a calcination process was needed in order to effectively use the waste in porcelain tile production. Therefore, the calcination process was applied to the colemanite solid waste before the waste-added bodies were sintered at 1210 °C and 1130 °C. The results were compared with those of the standard porcelain tile bodies produced at the same sintering temperatures. After detailed phase analysis (XRD), microstructural examination (SEM-EDX) and physical-mechanical tests, it was found that the standard porcelain tile body produced at 1210 °C (R1) could be obtained at 1130 °C by adding 5% colemanite solid waste (by weight) to the standard tile body to replace Na-feldspar (R7). This result enables production of porcelain tiles at lower temperatures without changing the other operational parameters, only using colemanite waste as a new fluxing agent in the body formulations.

**Key words:** Colemanite, Colemanite waste, Porcelain tile, Sintering agent.

### Introduction

Porcelain tiles have become one of the most important products of the ceramic industry in the last decade mainly because of their attractive physical and mechanical properties including high strength, high fracture toughness and density, excellent chemical resistance and low water absorption [1]. These products are generally sintered at 1200 °C or even at a slightly higher temperature and the formulations are mainly comprised of large amounts of Na-feldspar, K-feldspar, talc and fluxing agents such as glass-ceramic frits together with clay, kaolin and silica sand in lesser amounts [2]. The microstructure of the sintered porcelain tiles possesses quartz and mullite crystals in a glassy matrix depending on the chemical composition of the formulations [3]. The microstructure directly affects the technical properties of the final product [4]. Therefore, it is necessary to use good quality raw materials of higher purity in the starting composition in order to produce porcelain tiles with the desired technical

specifications and microstructural properties. These good quality raw materials are not only needed for the production of porcelain tiles but also for other ceramic tiles (wall and floor) and even for glass wares. Because of the high demand and the cost of the current raw materials in this industry, alternative materials research has increased. Many wastes have been tested by the ceramic industry as alternative economical raw materials [5-12].

Borates are generally known as natural materials containing  $\text{B}_2\text{O}_3$  and they have been used by the ceramic industry for centuries owing to the fact that they have glass-forming properties and reduce the melting point of the glassy phase formed in ceramic bodies [13]. There are over 200 naturally occurring boron-containing minerals but the most commercially important and frequently traded minerals are tincal ( $\text{Na}_2\text{B}_4\text{O}_7\cdot 10\text{H}_2\text{O}$ ), colemanite ( $\text{Ca}_2\text{B}_6\text{O}_{11}\cdot 5\text{H}_2\text{O}$ ), ulexite ( $\text{NaCaB}_5\text{O}_9\cdot 8\text{H}_2\text{O}$ ) and kernite ( $\text{Na}_2\text{B}_4\text{O}_7\cdot 4\text{H}_2\text{O}$ ). World boron reserves are located mainly in Turkey (72%), the United States (6.8%), Russia (8%), Chile (3.50%) and China (3.2%). Boron mining and processing activities have been carried out by the National Boron Board (Eti Mine) in Turkey as a monopoly by law. Eti Mine produces concentrated and refined products of tincal, colemanite and ulexite in Turkey. The production of boron chemicals was planned to reach 1,063 million

\*Corresponding author:  
Tel : +274 2652031-4307  
Fax: +274 2652066  
E-mail: nezahatediz@hotmail.com

tons in 2007 by Eti Mine. The Emet Colemanite Mine of the National Boron Board of Turkey (Eti Mine) located in Emet Town of Kütahya Province was established in 1958. It produces concentrated colemanite by processing the ore excavated from "Espey" and "Hisarcık" districts. It also produces boric acid in its recently-constructed plant with a production capacity of 100,000 tonnes/year. The colemanite waste used in the research was taken from the concentrator plant of Hisarcık District and a large amount of wastes are produced during both mining and boron processing operations [14]. According to the technical office of the Emet Colemanite Mine, the amount of ore processed and the total waste production were 610,000 tonnes and 329,983 tonnes, respectively in 2007 at Hisarcık Concentrator. The amounts of colemanite solid wastes in this total were 329,983 tonnes. It is, therefore, very important to make use of the wastes to both protect the environment and create increased revenue.

After investigating previous studies related to boron-bearing solid wastes, it was seen that most of the research on using boron wastes in the ceramic industry was focused on the tincal ( $\text{Na}_2\text{B}_4\text{O}_7 \cdot 10\text{H}_2\text{O}$ ) containing wastes [15-27] whereas colemanite ( $\text{Ca}_2\text{B}_6\text{O}_{11} \cdot 5\text{H}_2\text{O}$ ) containing wastes were mainly studied for possible use in the cement industry [28-31]. Another significant point in these studies is that the final product is found to have a considerable degree of deformation if boron-bearing solid wastes are used in high weight percentages in ceramic tile body formulations in fast firing tile production conditions. However, although some explanation could be offered for this deformation, there is no clear evidence why this deformation occurred in fast-firing tile bodies after sintering. By considering these reasons mentioned, it is thought that boron-bearing solid wastes should be calcinated in order to avoid deformation problems after sintering.

Therefore, the purpose of this research is to investigate the possible use of colemanite solid wastes (calcinated and raw) in porcelain tile production as an alternative fluxing agent to Na-feldspar and to explain the protective effects of the calcination process from the deformation which occurred when there is boron-bearing minerals in porcelain tile body formulations. If this aim is made possible, then the ceramic industry will benefit by having a new and cheaper raw material in porcelain tile production and it will provide clear evidence for the reasons of deformation occurring after sintering.

## Experimental Studies

### Calcination process

The calcination process was applied to the raw colemanite solid waste which was ground in a ring mill for 1 minute, using a furnace (Naberham Program Controller C19). The furnace conditions were so arranged that 500 °C was reached at a heating rate of 5 °C minute<sup>-1</sup> and the samples were then cooled down to room temperature at a cooling rate of 5 °C minute<sup>-1</sup> after a one hour standing

period at 500 °C.

The raw colemanite solid waste was called calcined colemanite solid waste after the calcination process was completely finished and it was coded CCSW while the raw colemanite solid waste was coded RCSW throughout the research.

### Characterization of the materials used

In order to prepare the porcelain tile recipes, Na-feldspar, K-feldspar and 3 different clays and siliceous (quartz) sand were used as the starting raw materials. Semi-quantitative chemical analysis of the raw materials was made using an X-ray fluorescence (XRF) instrument (Spektro X-Lab 2000). The chemical analysis of CCSW and RCSW was made using an inductive coupled plasma (ICP) instrument (Perkin Elmer Optima 3000) and an energy dispersive X-ray (EDX) spectrometer (Oxford Instruments 7430) with a polymer-based ultra thin window (UTW) since the wastes contained boron oxides.

The phase analysis of CCSW and RCSW was made by X-ray diffractometers (Rigaku Miniflex ZD13113 and Rigaku Rint 2000 series) using  $\text{CuK}_\alpha$  X-rays ( $\lambda = 1.54056 \text{ \AA}$ ) in the range of 5-70° at a rate of 1°/minute in order to determine the mineral content of the material after calcination. The thermal behaviours of the CCSW and RCSW were investigated through a differential thermogravimetric analysis instrument (Inseis Thermowage L81) at a rate of 10 °C minute<sup>-1</sup> up to 600 °C. The thermal behaviour of the wastes with increasing temperature were determined using the DTA and TG curves and the results were also used as preliminary data for a successful calcination process.

In order to determine the effectiveness of the calcination process, the particle size distributions of RCSW which was ground in a ring mill for 1 minute and CCSW obtained after the calcination process were determined using a light scattering laser diffractometer (Malvern Instruments hydro 2000G). The validity of the results for CCSW was also controlled by a field emission gun scanning electron microscope (Zeiss FEG-SEM Supra 50 VP).

### Porcelain tile body recipes with RCSW and CCSW and their characterization

Reference (R1) and RCSW-added (R1, R2, R3, R4 and R5) new porcelain tile body recipes were prepared for the research. In order to find out the suitability of RCSW-added recipes for porcelain tile production, the sintering behaviour and transition temperatures were determined using an optical dilatometer (Misura 332-ODHT-HSM 1600/80). By considering the optical dilatometer results of reference (R1) and RCSW-added (R1, R2, R3, R4 and R5) new porcelain tile body recipes, new reference (R6) and CCSW-added (R7) porcelain tile body recipes were formed so that the effects of the CCSW addition could be determined and to find the differences between the sintering behaviour of RCSW and CCSW.

### Porcelain tile production method and the tests applied

The process flowchart for the production of porcelain tiles using the recipes coded R1-R7 is given in Fig. 1. Every stage of the production explained in Fig. 1 was carried out under factory conditions in order to investigate a truly industrial application of the colemanite wastes. The physical-mechanical properties of the green and fired porcelain tile bodies with both RCSW and CCSW were determined according to standard methods [32-33]. Three specimens were used for each test carried out to secure the reliability of the results.

### Characterization of the sintered bodies with RCSW and CCSW

In order to find out the phase transitions of the reference, RCSW and CCSW-added porcelain tile bodies after sintering, X-ray diffraction (XRD) analysis (Rigaku Miniflex ZD13113 and Rigaku Rint 2000) was made on powdered samples. Microstructural analysis was also made in order to examine the changes in the microstructure of the porcelain tile bodies after sintering. The surfaces of the porcelain tile bodies, which were prepared through

conventional sample preparation methods (cutting, mounting, polishing and etching) were coated with a thin gold layer using a sputtering technique (Agar sputter coater) in order to prevent charging during microstructural analysis. Microstructural investigations were made using a field emission electron gun scanning electron microscope (Zeiss Supra FEG-SEM 50 VP), attached to an ultra thin window (UTW) energy dispersive X-ray spectrometer (Oxford Instruments 7430 EDX).

## Results and Discussion

### Results of characterization of the materials used

Semi-quantitative chemical analysis of the materials used in the reference, RCSW and CCSW-added porcelain tile bodies is given by Table 1. When chemical analysis of the RCSW and CCSW are examined, it is seen that these wastes contain high amounts of fluxing oxides ( $B_2O_3$ ,  $K_2O$ ,  $Na_2O$  and  $Fe_2O_3$ ) and earthy alkali oxides such as  $MgO$  and  $CaO$  which play an important role in the vitrification behaviour and ease liquid phase occurrence during sintering. Mineralogical phase analyses of RCSW

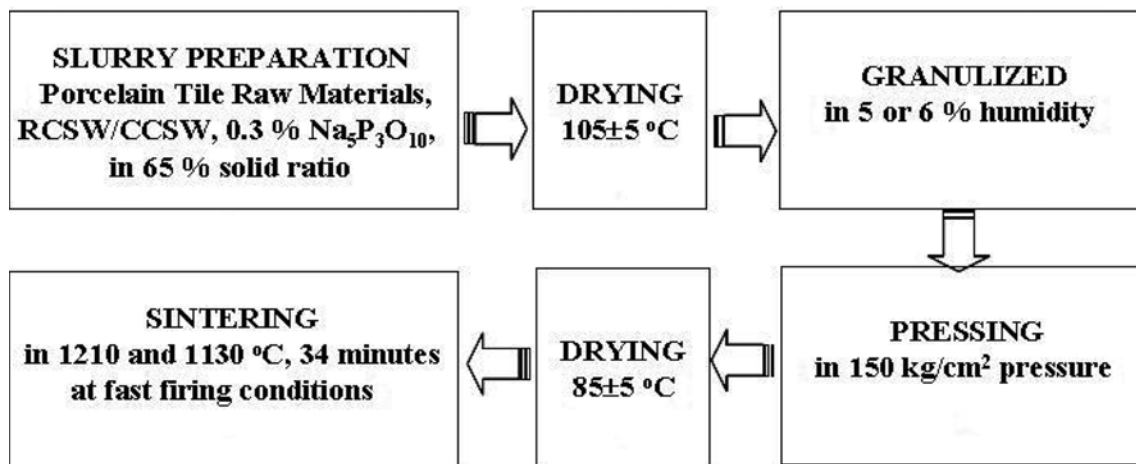
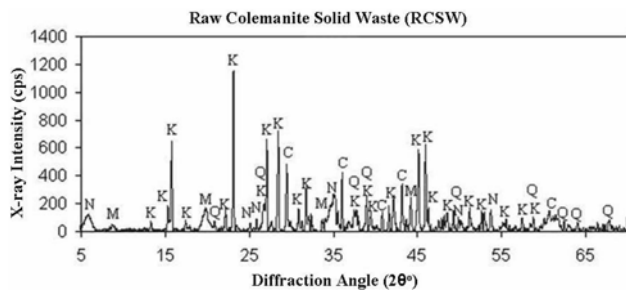


Fig. 1. Production method for porcelain tiles.

Table 1. Chemical analysis of the materials used (weight %)

Oxides	Clay-1	Clay-2	Clay-3	Na-Feldspar	K-Feldspar	Silica Sand	RCSW	CCSSW
SiO <sub>2</sub>	8.58	62.75	60.65	67.41	73.44	91.36	23.03	24.10
Al <sub>2</sub> O <sub>3</sub>	1.17	23.24	26.28	20.65	17.66	5.42	7.22	12.58
Fe <sub>2</sub> O <sub>3</sub>	0.50	2.25	0.95	0.24	0.54	0.30	3.11	3.62
TiO <sub>2</sub>	0.07	1.22	1.34	0.50	0.10	0.21	0.25	0.46
CaO	3.74	0.12	0.24	0.39	0.11	0.05	14.98	16.99
MgO	39.80	0.73	0.58	0.19	0.19	0.03	7.37	10.78
Na <sub>2</sub> O	0.72	0.40	0.68	6.55	3.22	0.10	0.06	0.09
K <sub>2</sub> O	0.11	2.44	2.34	3.62	4.24	1.08	2.10	3.59
B <sub>2</sub> O <sub>3</sub>	-	-	-	-	-	-	21.25	27.79
*LOI	45.31	6.85	6.94	0.45	0.50	1.45	20.98	-
TOTAL	100	100	100	100	100	100	100	100

\*Loss on Ignition



**Fig. 2.** XRD analysis of RCSW [N = Natronite-15A :  $\text{Na}_{0.3}\text{Fe}_2\text{Si}_4\text{O}_{10}(\text{OH})_2 \cdot 4\text{H}_2\text{O}$ , M = Muscovite :  $\text{KAl}_2\text{Si}_3\text{AlO}_{10}(\text{OH})_2$ , K = Colemanite :  $\text{Ca}_2\text{B}_6\text{O}_{11} \cdot 5\text{H}_2\text{O}$ , Q = Quartz :  $\text{SiO}_2$ , C = Calcite :  $\text{Ca}(\text{CO}_3)$ ].

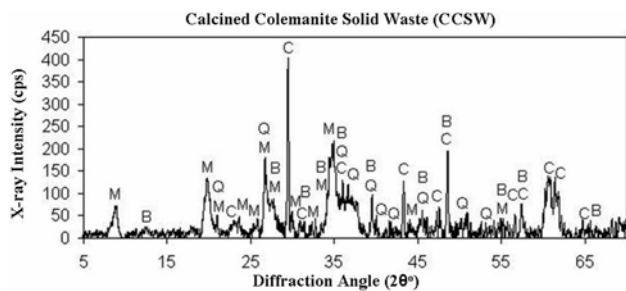


**Fig. 3.** XRD analysis of CCSW [M = Muscovite :  $\text{KAl}_2\text{Si}_3\text{AlO}_{10}(\text{OH})_2$ , Q = Quartz :  $\text{SiO}_2$ , C = Calcite :  $\text{Ca}(\text{CO}_3)$ , B = Boron oxide :  $\text{B}_2\text{O}_3$ ].

and CCSW are given in Fig. 2 and 3, respectively. It is seen from these figures that phases of muscovite [ $\text{KAl}_2\text{Si}_3\text{AlO}_{10}(\text{OH})_2$ ], quartz [ $\text{SiO}_2$ ] and calcite [ $\text{Ca}(\text{CO}_3)$ ] are common mineralogical phases of RCSW and CCSW. However, natronite-15A [ $\text{Na}_{0.3}\text{Fe}_2\text{Si}_4\text{O}_{10}(\text{OH})_2 \cdot 4\text{H}_2\text{O}$ ] and colemanite [ $\text{Ca}_2\text{B}_6\text{O}_{11} \cdot 5\text{H}_2\text{O}$ ] phases seen in RCSW were not observed in the CCSW mineralogical phase structure owing to the loss of water molecules after calcination at 500 °C [34]. On the other hand, boron oxide [ $\text{B}_2\text{O}_3$ ] was only seen in the mineralogical phase structure of CCSW (Fig. 3) which can be explained by decomposition of the colemanite at 500 °C [34]. This result gives the first indication of the success in the calcination process applied.

DTA/TG curves of RCSW and CCSW are seen in Fig. 4 and 5, respectively. When the thermal behaviour of RCSW was examined (Fig. 4) an endothermic peak was seen at 70.8 °C owing to the loss of physically bonded water in the DTA curve. When the TG curve at 70.8 °C was examined it was seen that there was a weight loss of 4.94%. As can be seen from the endothermic peaks of the DTA curve at 295.1 °C and 374.6 °C, 5 molecules of water chemically bonded to the colemanite mineral of RCSW were removed in two stages. The weight loss of 39.76% that occurred at this point is easily seen from the TG curve. The results of the DTA analysis applied to the colemanite waste shows great similarity to those of the pure colemanite mineral [35-36]. The weight loss of 2.78% seen on the TG curve at 400-600 °C can be considered as an indication of the removal of crystal water existing in clay minerals such as natronite

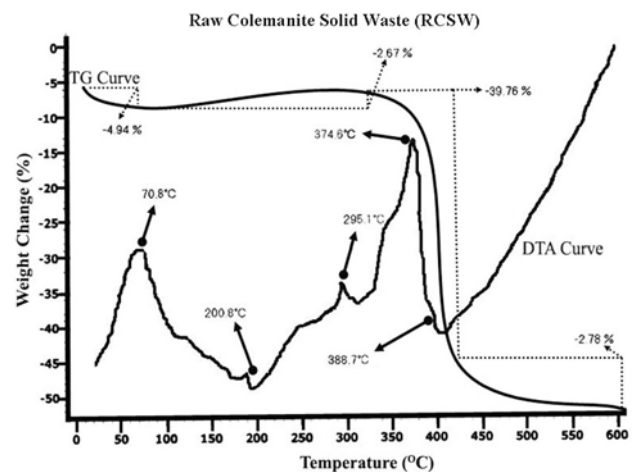


**Fig. 4.** DTA and TG analysis of RCSW.

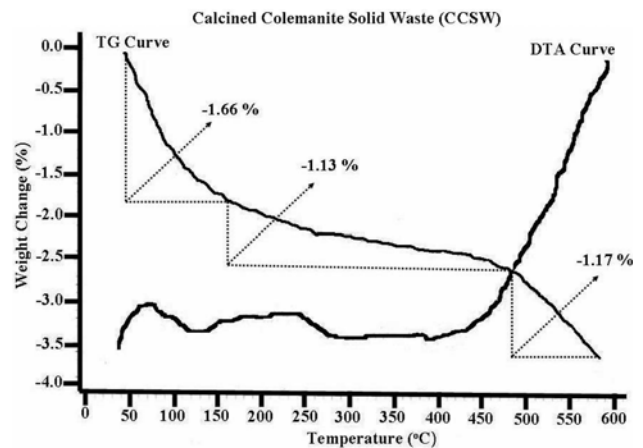


**Fig. 5.** DTA and TG analysis of CCSW.

and muscovite, Fig. 4 [37].

Since sudden gas removal from RCSW in Fig. 4 was determined from DTA/TG analysis at 0-400 °C and this would cause a porcelain tile body to be deformed, it was decided to apply calcination to RCSW at 500 °C. When DTA/TG curves of CCSW were examined (Fig. 5), it was noticed that there was a weight loss of 1.66% between 50 °C and 100 °C. This weight loss was due to the removal of physically adsorbed water molecules during the analysis. Moreover, it was observed that there was a weight loss of 1.13% between 100 °C and 500 °C in CCSW (Fig. 5). Considering the weight loss of RCSW at the same temperature range (100-500 °C) which was given in Fig. 4 as 42.43%, the weight loss of CCSW (only 1.13%) can be regarded as very small which is a second indication that the calcination operation was successful.

The weight loss of CCSW at 500 °C which was 1.17% as derived from DTA/TG curve originated from clay minerals such as muscovite in CCSW. Because clay minerals such as muscovite lose their crystal water at about 500 °C [37] which was the calcination temperature, chemical reactions within these minerals in CCSW are inevitable.

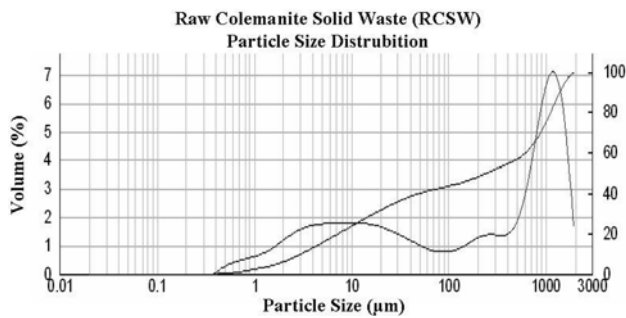


Fig. 6. Particle size distribution of RCSW.

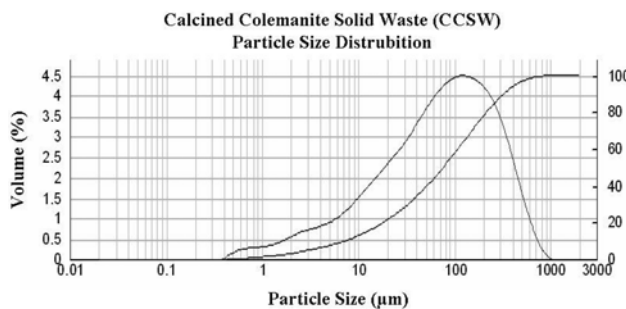


Fig. 7. Particle size distribution of CCSW.

The results of particle size analyses of RCSW and CCSW which were determined by a light scattering laser diffractometer are given in Figs. 6 and 7, respectively.

In order to increase the efficiency of calcination, RCSW was ground in a ring mill for 1 minute to increase the specific surface area of the particles for an easier removal of water molecules [38]. After the milling operation, the particle size distribution of RCSW was determined as  $d(0.1) = 3 \mu\text{m}$ ,  $d(0.5) = 245 \mu\text{m}$  and  $d(0.9) = 1406 \mu\text{m}$  (Fig. 6). This result revealed that RCSW did not have a homogeneous particle size distribution and the average particle size was  $245 \mu\text{m}$ .

After calcination the particle size distribution of CCSW was found to be  $d(0.1) = 7.2 \mu\text{m}$ ,  $d(0.5) = 76 \mu\text{m}$  and  $d(0.9) = 322 \mu\text{m}$  (Fig. 7). It can be said that calcined colemanite solid waste had a homogeneous particle size distribution and the average particle size was  $76 \mu\text{m}$  after calcination. This was accepted as a third indication

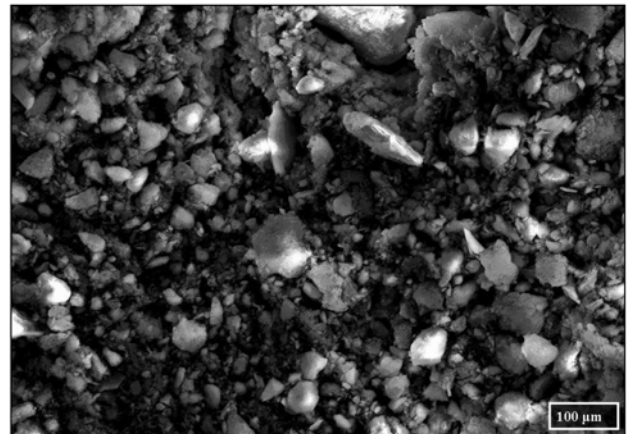


Fig. 8. SEM image of CCSW.

of a successful calcination operation. The particle size distribution of CCSW determined by the light scattering laser diffractometer was also confirmed by secondary electron SEM images. As can be seen from Fig. 8, the SEM image also proves that CCSW had a homogeneous particle size distribution.

After the chemical, XRD and DTA/TG analyses, it was understood that colemanite-bearing wastes (RCSW and CCSW) could be used as an alternative fluxing agent for feldspar in porcelain tile production.

#### Evaluation of the recipes with RCSW and CCSW by considering results of optical dilatometer characterization

The chemical composition of the rich oxide content is not the only criteria for a material to be used in porcelain tile production; the possible reactions of the alternative raw material with the other body constituents during the firing and sintering behaviour are also important. Therefore, the sintering behaviour in a fast-firing environment of the reference (R1) and RCSW-added porcelain tile bodies (R2, R3, R4 and R5) whose rational compounds are given in Table 2 were examined through an optical dilatometer to show whether they were suitable raw materials.

The detailed optical dilatometer results of the reference and RCSW-added porcelain tile bodies are given in

Table 2. Rational compositions of the reference R1 and RCSW-added R2, R3, R4, and R5 porcelain tile bodies

Rational Analysis	R1 (weight %)	R2 (weight %)	R3 (weight %)	R4 (weight %)	R5 (weight %)
Na-feldspar	32.1	27.1	22.1	17.1	12.1
RCSW	-	5.0	10.0	15.0	20.0
K-feldspar	10.0	10.0	10.0	10.0	10.0
Silica sand	9.0	9.0	9.0	9.0	9.0
Clay-1	1.7	1.7	1.7	1.7	1.7
Clay-2	22.1	22.1	22.1	22.1	22.1
Clay-3	25.1	25.1	25.1	25.1	25.1
TOTAL	100.0	100.0	100.0	100.0	100.0

Fig. 9. When this figure is examined, it is seen that there was a sudden expansion in RCSW-added bodies compared to the reference body at 350 °C-450 °C. This expansion was caused by the removal of 5 molecules of water within the colemanite mineral of RCSW with increasing temperature [34]. The increase in the amount of RCSW also causes a linear increase in the expansion rate at 350 °C-450 °C.

However, the samples could not remain for a long period at 350 °C-450 °C since this is not part of the fast-firing operation applied in porcelain tile production. Therefore, porcelain tile bodies with RCSW will undergo deformation if they are to be fired at the reference body sintering temperature owing to the occurrence of severe gas reactions by the decomposition of colemanite mineral at 350 °C-450 °C, as seen from Fig. 9.

Moreover, it was observed that sintering temperatures of RCSW-added bodies were reduced compared to that of the reference body as a function of the RCSW addition (R1 = 951 °C, R2 = 876 °C, R3 = 835 °C, R4 = 813 °C, R5 = 786 °C). The reason can be explained by an increase in fluxing of alkali or earth alkali oxides such as B<sub>2</sub>O<sub>3</sub>, Fe<sub>2</sub>O<sub>3</sub>, K<sub>2</sub>O, CaO and MgO with an increase of the RCSW addition [39]. However, these oxides decrease the viscosity of the glassy phase and hence cause bloating and deformation by carrying the gas bubbles to the surface at the sintering stage [40].

The sintering temperature applied to the reference bodies (R1) was 1210 °C under factory conditions. It is clearly seen from the transition points of the optical dilatometer curves that this temperature is rather high for the RCSW-added bodies (R2, R3, R4 and R5). Therefore, RCSW-added bodies of R2, R3, R4 and R5 will deform owing to the occurrence of excessive liquid phase if they are fired above 1170 °C, 1100 °C, 1050 °C and 980 °C, respectively. Using the results from the optical dilatometer, it was decided not to use RCSW-added R3, R4 and R5 recipes and only use RCSW-added R2 recipe.

In order to determine the sintering temperature of

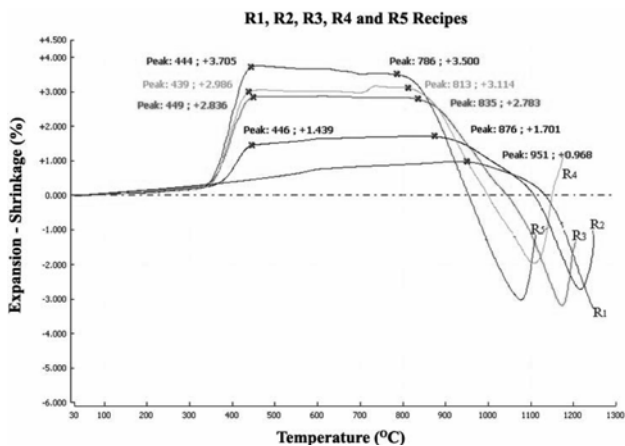


Fig. 9. Results from an optical dilatometer for the standard and the RCSW-added porcelain tile bodies.

RCSW-added R2 recipe, the bloating behaviour at maximum sintering temperatures of 1160 °C, 1170 °C and 1180 °C was examined by an optical dilatometer (Fig. 10). As can be seen from Fig. 10, the body was bloated at 1180 °C and shrank by 4.911% and 5.472% at 1160 °C and 1170 °C, respectively. Therefore, 1160 °C was chosen as the optimum sintering temperature for the R2 recipe since it yielded the maximum shrinkage value of 5.472%. There is still a need for an optimization of a new porcelain tile recipe owing to the sudden expansion of 1.829% originating from the decomposition of colemanite at 350 °C-450 °C. This need leads to calcination of RCSW above 500 °C as demonstrated by the results of the optical dilatometer shown in Figs. 9 and 10 as well as the DTA analysis given by Fig. 4. The expected result from the calcination above 500 °C was to avoid excessive gas accumulation owing to the decomposition of colemanite mineral at 350 °C-450 °C and therefore prevent these gases being transferred into the porcelain tile production stage to obtain un-deformed products.

The rational compounds of the new reference (R6) and CCSW-added (R7) porcelain tile recipes are given in Table 3. Although the optical dilatometer results showed that the optimum sintering temperature was 1160 °C, the nearest possible temperature of 1130 °C could only be applied to these new porcelain tile recipes (R6 and R7) under factory conditions. Besides, in order to control

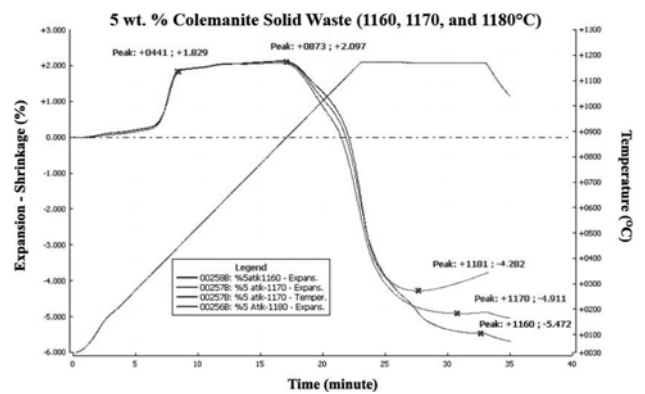


Fig. 10. Results from an optical dilatometer for the RCSW-added R2 bodies sintered at 1160 °C, 1170 °C and 1180 °C.

Table 3. Rational composition of the reference R6 and CCSW added R7 porcelain tile bodies

Rational Analysis	R6 (weight %)	R7 (weight %)
Na-feldspar	32.1	27.1
CCSW	-	5.0
K-feldspar	10.0	10.0
Silica sand	9.0	9.0
Clay-1	1.7	1.7
Clay-2	22.1	22.1
Clay-3	25.1	25.1
TOTAL	100.0	100.0

**Table 4.** Test results of the reference R1 and RCSW-added R2 bodies sintered at 1200 °C and the reference R6 and CCSW-added R7 bodies sintered at 1130 °C

Recipe Codes	Sintering Temperature (°C)	Dry Shrinkage (%)	Fired Shrinkage (%)	Green Strength (N/mm <sup>2</sup> )	Dry Strength (N/mm <sup>2</sup> )	Fired Strength (N/mm <sup>2</sup> )	Water Absorption (%)
R1	1210	0.91	10.55	0.83	3.12	32.73	0.10
R2	1210	1.32	13.87	0.91	3.58	20.24	1.44
R6	1130	0.88	6.65	0.79	3.01	20.86	4.18
R7	1130	1.07	12.37	0.86	3.17	30.86	0.63

the validity of the optimizations of recipes and to show the necessity of the calcination process, reference (R1) and RCSW-added (R2) porcelain tile recipes were sintered at 1210 °C although it was known that the (R2) porcelain tile recipe should have been sintered at 1160 °C, the optimum sintering temperature determined by the optical dilatometer.

#### Physical-mechanical tests applied to the RCSW and CCSW-added bodies

The results of physical-mechanical tests such as dry shrinkage, fired shrinkage, green strength, dry strength, fired strength and water absorption applied to the reference (R1) and RCSW-added (R2) bodies sintered at 1210 °C, and to the reference (R6) and CCSW-added (R7) bodies sintered at 1130 °C are given in Table 4.

From the table, it is seen that dry shrinkage, green strength and dry strength of green bodies of R2 and R7 (with RCSW and CCSW) bodies are increased compared to those of R1 and R6 (reference) bodies. The reason can be explained by the existence of clay minerals such as muscovite in the mineralogy of RCSW and CCSW which act as an organic binder in the un-sintered porcelain tile body [41].

The RCSW-added R2 body sintered at 1210 °C showed a higher fired shrinkage and water absorption but lower fired strength than reference R1 body.

The reason for the higher fired shrinkage could be explained by the fact that the glassy phase caused by the high fluxing oxides such as B<sub>2</sub>O<sub>3</sub>, K<sub>2</sub>O and Fe<sub>2</sub>O<sub>3</sub> in RCSW showed volumetric changes during cooling. Moreover these high fluxing oxides reduced the viscosity of the glassy phase which occurred by sintering at 1210 °C and caused a bloating effect in the R2 body. This resulted in body deformation in R2 and the fired strength of R2 (20.24 N/mm<sup>2</sup>) was found to be substantially lower than that of R1 body (32.73 N/mm<sup>2</sup>). It was known that the sintering temperature of 1210 °C was too high for R2 body and it would not be possible to obtain an un-deformed body at this temperature from the optical dilatometer result given in Fig. 9. So this experimental result confirmed the optimum sintering temperature of 1160 °C which was found by the optical dilatometer analysis for R2 body (Fig. 10).

The reason why water absorption of the R2 body (1.44%) was found to be higher than that of R1 (0.10%) was explained by an increase in the number of pores because of the bloating effect of sintering at 1210 °C.

The reason why the R7 body with CCSW had a higher fired shrinkage than that of the R6 body (both sintered at 1130 °C), on the other hand, was explained by the existence of a large amount of fluxing alkali and earth alkali type of oxides [39] within the CCSW (Table 1).

The fired strength of the reference R6 body (20.86 N/mm<sup>2</sup>) sintered at 1130 °C was found to be lower than that of the reference R1 body (32.73 N/mm<sup>2</sup>) sintered at 1210 °C. This can be explained by the fact that Na and K-feldspars which provide vitrification in the body could not melt adequately at the sintering temperature of 1130 °C and therefore they were unable to form the glassy phase [42]. This approach was confirmed by the findings of the optical dilatometer which proved the optimum sintering temperature for the R1 body had to be approximately 1200 °C (Fig. 9).

However, the fired strength of the R7 body with CCSW (30.86 N/mm<sup>2</sup>) sintered at 1130 °C was found to be much higher than that of the R6 body sintered at the same temperature (20.86 N/mm<sup>2</sup>). The fired strength of the R7 body with CCSW (30.86 N/mm<sup>2</sup>) sintered at 1130 °C was found to be quite similar to that of the R1 body sintered at 1210 °C (32.73 N/mm<sup>2</sup>).

The reason was explained by the fact that calcination of RCSW at 500 °C prevented sudden gas removal from the decomposition of the colemanite mineral at 350-450 °C and also the transfer of these gases to the sintering stage and the high fluxing oxides in the CCSW provided a homogeneous vitrification in the sintering stage. This result is confirmed by the finding of the optical dilatometer which showed that the optimum sintering temperature for the R2 body would be 1160 °C and calcination was a necessity for RCSW in order to produce un-deformed porcelain tile bodies (Fig. 10).

#### Characterization results of sintered bodies with RCSW and CCSW

##### XRD phase analysis results

XRD analysis was carried out in order to determine the phase changes in reference body R1 and R2 body with RCSW sintered at 1210 °C as well as reference R6 body and R7 body with CCSW sintered at 1130 °C, after the sintering operation. Comparison of the XRD results of R1 and R2 with RCSW is given in Fig. 11. When Fig. 11 is examined, it is seen that the main

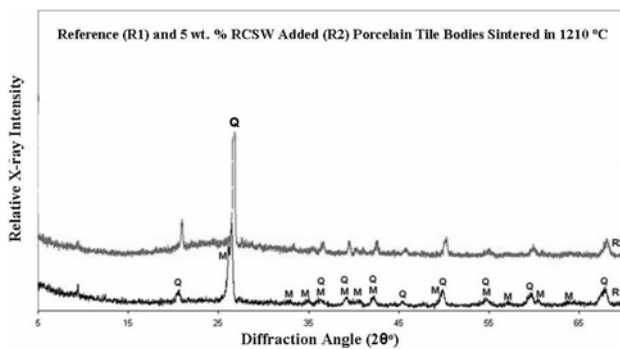


Fig. 11. XRD Results of R1 and R2 bodies sintered at 1210 °C.

phases in the R1 reference porcelain tile body are quartz ( $\text{SiO}_2$ ) and mullite ( $3\text{Al}_2\text{O}_3 \cdot 2\text{SiO}_2$ ). When R2 is examined, it is seen that no new phase is introduced with the RCSW addition, although the intensity of the mullite phase is reduced. In other words, the amount of mullite in the porcelain tile body was reduced qualitatively after an RCSW addition to the system. This result can be explained by the dissolution of mullite in a glassy phase of low viscosity created by the high alkali fluxing type of oxides such as  $\text{B}_2\text{O}_3$  with the introduction of RCSW to the system [43].

A comparison of XRD results of the reference R6 body and R7 body with CCSW sintered at 1130 °C is given in Fig. 12. When Fig. 12 is examined it is seen that reference R6 body has quartz ( $\text{SiO}_2$ ) and anorthoclase [ $(\text{Na},\text{K})\text{Si}_3\text{AlO}_8$ ] phases. The anorthoclase phase found in reference R6 porcelain body after sintering indicated that a sintering temperature of 1130 °C was not adequate for this body. As a matter of fact, the fired strength of R6 body was found to be rather low and optical dilatometer analysis indicated that the optimum sintering temperature for the R1 reference body would be approximately 1200 °C (Fig. 9).

When the R7 body is examined it is clearly seen that the intensity of the anorthoclase phase is reduced and the reason can be explained by the addition of CCSW. In other words, the anorthoclase phase is dissolved in the glassy phase occurring in the sintering stage. Alkali

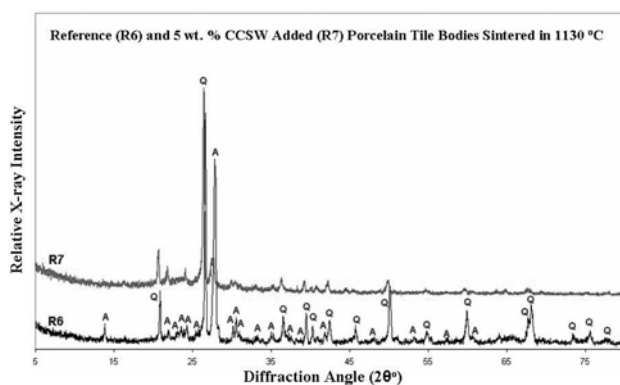


Fig. 12. XRD results of R6 and R7 bodies sintered at 1130 °C.

and earth alkali fluxing oxides such as  $\text{B}_2\text{O}_3$ ,  $\text{Fe}_2\text{O}_3$ ,  $\text{K}_2\text{O}$ ,  $\text{CaO}$  and  $\text{MgO}$  within the CCSW reduced the melting point of the anorthoclase phase by reducing the temperature of occurrence of the glassy phase.

The vitrification rate was increased by having a lower viscosity due to the oxides present in the liquid phase. This enabled the anorthoclase phase to be dissolved in the glassy phase at a lower temperature. This result indicated that a sintering temperature of 1130 °C would be adequate with the addition of CCSW for the bodies which did not receive an adequate vitrification at the sintering temperature of 1210 °C.

### Microstructural characterization and its relationship with physical-mechanical properties

Microstructural changes in porcelain tile bodies of R1, R6 (sintered at 1210 °C and 1130 °C), R2 with RCSW (sintered at 1210 °C) and R7 with CCSW (sintered at 1130 °C) were examined with a scanning electron microscope (SEM) and an energy dispersive X-ray (EDX) spectrometer. When the scanning electron microscope (SEM) image of the reference R1 body shown in Fig. 13(a) is examined, it can be said that the dark grey areas reflect the glassy matrix phase, whereas black areas indicate the pores. From this image, it can easily be said that the reference R1 body has a homogeneous matrix structure and very few pores. This result was regarded as the reason for the low water absorption value obtained (0.10%) from the reference R1 body. Moreover, it is seen that there are some large grains distributed and dissolved within the glassy matrix phase when the SEM image is carefully examined. In order to

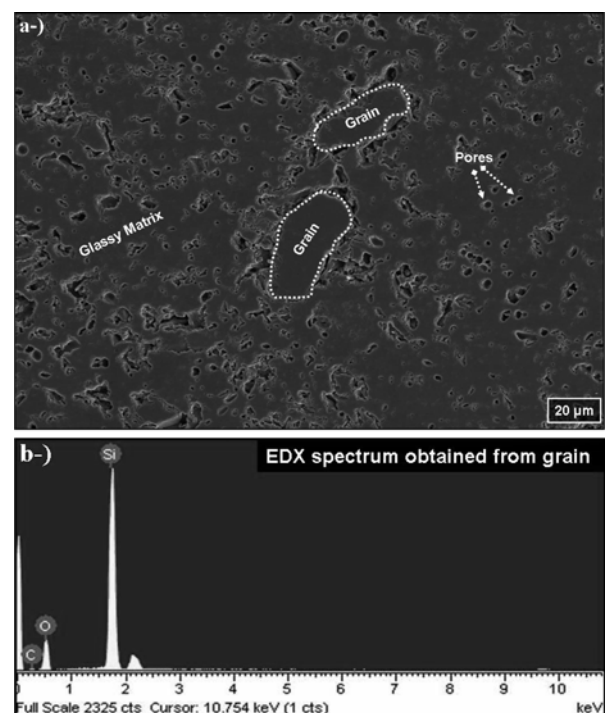
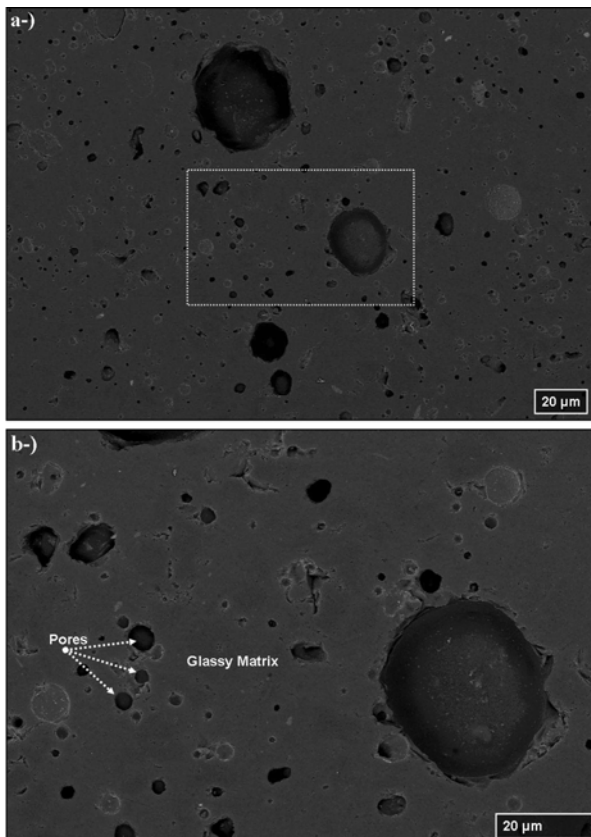


Fig. 13. (a) SEM image of the R1 standard porcelain tile body sintered at 1210 °C; (b) EDX spectrum indicating  $\text{SiO}_2$  phase.

determine the phase or phases, the grains belong to, energy dispersive X-ray (EDX) analysis was carried out. According to the EDX spectrum given in Fig. 13(b), it can be said that these grains belong to the quartz ( $\text{SiO}_2$ ) phase. This result supported the idea that the reference R1 porcelain tile body is predominantly comprised of the quartz ( $\text{SiO}_2$ ) phase as can be seen from the result of the XRD analysis applied to the R1 body as well as low concentrations of the mullite phase (Fig. 11). Moreover, the reason for the high fired strength of the R1 body ( $32.73 \text{ N/mm}^2$ ) can be explained by the existence of the quartz ( $\text{SiO}_2$ ) phase distributed within the matrix phase as well as the mullite ( $3\text{Al}_2\text{O}_3 \cdot 2\text{SiO}_2$ ) phase according to the SEM-EDX and XRD analyses, respectively [4]. The reason of the low concentrations of the mullite phase formation in porcelain tile bodies could be explained by considering changeable starting composition characteristics, fast firing cycle and low firing temperature in porcelain tile production [4]. The results related to the microstructure of the standard porcelain tile were in good agreement with the findings of previous studies [44-45].

In order for the R1 body to pose the homogeneous matrix structure shown in the SEM image (Fig. 13(a)), the optimum sintering temperature for this body should be approximately  $1200^\circ\text{C}$  according to the results of the optical dilatometer given in Fig. 9. When the RCSW-added R2 body is examined (Fig. 14(a), and (b)), it is



**Fig. 14.** (a) SEM image of the RCSW-added R2 body sintered at  $1210^\circ\text{C}$ ; (b) Detailed SEM image of the area indicated in Fig. 14(a).

seen that the body has a considerable amount of pores in its microstructure and deformation after sintering. This is explained by the bloating effect at the sintering stage owing to the fluxing effect of alkali and earth alkali oxides such as  $\text{B}_2\text{O}_3$ ,  $\text{Fe}_2\text{O}_3$ ,  $\text{K}_2\text{O}$ ,  $\text{CaO}$  and  $\text{MgO}$  within the chemical and mineralogical compositions of RCSW and the transfer of intensive gas accumulating reactions resulting from the decomposition of the colemanite mineral ( $\text{Ca}_2\text{B}_6\text{O}_{11} \cdot 5\text{H}_2\text{O}$ ) to the sintering stage. The reason why the RCSW-added R2 body has a lower fired strength and higher water absorption values ( $20.24 \text{ N/mm}^2$  and  $1.44\%$ ) than those of the reference R1 body ( $32.73 \text{ N/mm}^2$  and  $0.10\%$ ) can easily be observed by examining the microstructures given in Fig. 14(a), and (b). As is well known, an increase in porosity generally results in a decreased fired strength and increased water absorption for ceramic bodies [46]. SEM images of the RCSW-added R2 body (Fig. 14(a), and (b)) prove that a firing temperature of  $1210^\circ\text{C}$  applied in the factory is too high as supported by the results of the optical dilatometer analysis given in Fig. 9. The excessive porosity and deformation seen in the microstructure of the RCSW-added porcelain tile bodies (Fig. 14(a), and (b)) necessitate the application of calcination to RCSW and to lower the sintering temperature from  $1210^\circ\text{C}$ .

An SEM image which was produced to understand the microstructural changes of the reference R6 porcelain body sintered at  $1130^\circ\text{C}$  is seen in Fig. 15(a). From Fig. 15(a), it is seen that the reference R6 body sintered at  $1130^\circ\text{C}$  is comprised of two different phases indicated by light grey and dark grey areas. In order to determine the chemical compositions of these phases, EDX analysis was applied to the related grains (Fig. 15(b) and (c)).

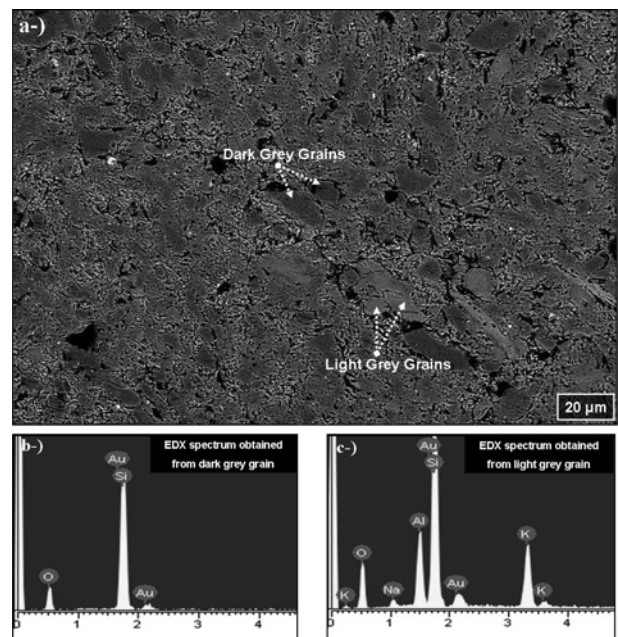


**Fig. 15.** (a) SEM image of the R6 body sintered at  $1130^\circ\text{C}$ ; (b) EDX spectrum indicating  $\text{SiO}_2$  phase (dark grey grain), (c) EDX spectrum indicating  $[(\text{Na}, \text{K})\text{Si}_3\text{AlO}_8]$  phase (light grey grain).

When the EDX spectrum given in Fig. 15(b) is examined, it is seen that the dark grey grain is comprised of Si and O elements. According to the EDX analysis (Fig. 15(b)), it can be said that this grain belongs to the quartz ( $\text{SiO}_2$ ) phase. As the EDX spectrum given in Fig. 15(c) is reviewed, it is realized that the light grey coloured grain is comprised of K, O, Na, Al and Si elements. According to the EDX analysis (Fig. 15(c)), it can be said that this grain belongs to the anorthoclase  $[(\text{Na,K})\text{Si}_3\text{AlO}_8]$  phase. Therefore, the results of the EDX analysis (Fig. 15(b) and (c)) supports the results of XRD analysis (Fig. 12) applied to the reference R6 porcelain tile body sintered at 1130 °C. The presence of the anorthoclase phase in the reference R6 porcelain tile body indicated that the sintering temperature applied was not sufficient and that the anorthoclase mineral was not dissolved in the glassy phase occurring at 1130 °C [42]. This result explains the reason why the fired strength of the reference R6 body sintered at 1130 °C (20.86 N/mm<sup>2</sup>) is much lower than that of reference R1 body sintered at 1210 °C (32.73 N/mm<sup>2</sup>). A homogeneous matrix structure to increase the strength of R6 body was not developed since the anorthoclase mineral was not dissolved at the sintering temperature of 1130 °C. Together with the results of microstructural analysis (Fig. 15(a), (b), and (c)), the optical dilatometer results (Fig. 9) also indicate that the optimum sintering temperature for reference R1 body should be around 1200 °C.

An SEM image and the results of the EDX analysis of the CCSW-added R7 porcelain tile body sintered at 1130 °C are given in Fig. 16(a), and (b), respectively.

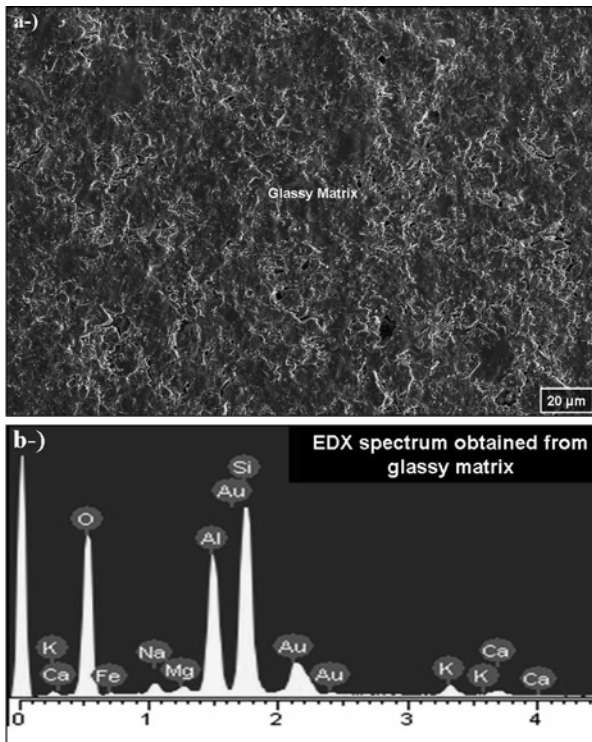


**Fig. 16.** (a) SEM image of the CCSW-added R7 body sintered at 1130 °C; (b) EDX spectrum indicating glassy matrix phase.

As Fig. 16(a) is examined, it is observed that the CCSW-added R7 porcelain tile body possesses a glassy compact matrix structure and sufficient vitrification in the body occurred. According to the EDX analysis made for chemical composition of the glassy matrix (Fig. 16(b)), K, Ca, O, Fe, Na, Mg, Al and Si elements existed in the glassy matrix. The presence of these elements in the glassy matrix indicates that the CCSW played an active role during sintering and sintering was accomplished successfully at 1130 °C. This result was also supported by the results of the optical dilatometer (Fig. 10) which indicated that the optimum sintering temperature for the R2 body should be 1160 °C.

The SEM images given in Fig. 17(a) and (b) explain that pores within the CCSW- added R7 porcelain tile body were mostly not open to the surface (closed pores) and were dispersed within the glassy matrix, independently vitrified in the body. Therefore, the SEM images presenting the homogeneous glassy matrix together with closed pores (Fig. 17(a) and (b)) reveal the reasons why the water absorption value of the CCSW-added R7 body sintered at 1130 °C (0.63%) is much lower than that of the reference R6 body sintered at the same temperature (4.18%) and the fired strength of the CCSW-added R7 body sintered at 1130 °C (30.86 N/mm<sup>2</sup>) is almost the same as that of the reference R1 body sintered at 1210 °C (32.73 N/mm<sup>2</sup>).

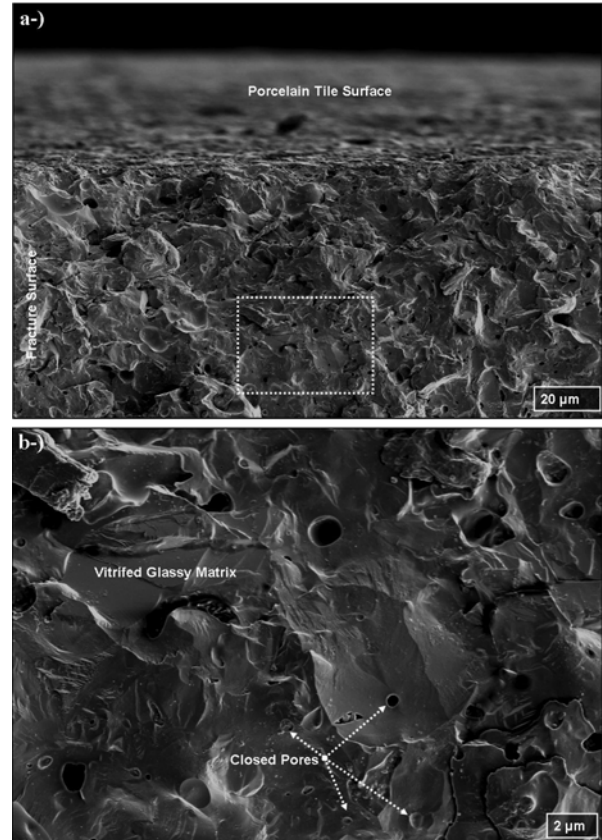


**Fig. 17.** (a) SEM image of the CCSW-added R7 body sintered at 1130 °C explaining the pore distribution; (b) Detailed SEM image of the area indicated in Fig. 17 (a).

In short, the microstructural observation of a homogeneous glassy matrix dissolving quartz and anorthoclase phases together with closed pores explains the reduced water absorption and increased fired strength values in the CCSW-added R7 body sintered at 1130 °C [4].

## Conclusions

In this research, the use of colemanite solid waste in fast firing porcelain tile production as an alternative fluxing agent to Na-feldspar was investigated without changing the process parameters of the factory. After detailed chemical and XRD analyses, it was found that the waste possessed important chemical and mineralogical phases for ceramic bodies such as  $B_2O_3$ ,  $K_2O$ ,  $Na_2O$ ,  $Fe_2O_3$ ,  $MgO$  and  $CaO$  for their fluxing character together with muscovite [ $KAl_2Si_3AlO_{10}(OH)_2$ ], quartz [ $SiO_2$ ], calcite [ $Ca(CO_3)$ ], natronit-15A [ $Na_{0.3}Fe_2Si_4O_{10}(OH)_2 \cdot 4H_2O$ ] and colemanite [ $Ca_2B_6O_{11} \cdot 5H_2O$ ]. This result showed that colemanite solid waste could be used as an alternative fluxing agent in porcelain tile bodies. From the DTA/TG analysis, on the other hand, it was noticed that colemanite solid waste lost 40% of its weight owing to the removal of the chemically-bonded 5 molecules of water corresponding to the endothermic peaks between 295 °C and 375 °C. It was then obvious that this weight loss corresponding to the decomposition of the colemanite mineral would cause body deformation when sintered in a fast firing condition. Therefore, an optical dilatometer analysis was carried out for the new bodies with colemanite waste and for the standard bodies to determine the sintering behaviour of the waste and to find out whether the weight losses that occurred at 295 °C-375 °C were transferred to the sintering stage.

When the optical dilatometer results were analyzed, it is seen that excessive reactions were transferred to the sintering stage which occurred during the decomposition of the colemanite mineral owing to the sudden expansion at 350 °C compared to the standard tile body. This result also explains the reason why the tile bodies with large amounts of tincal mineral ( $Na_2B_4O_7 \cdot 10H_2O$ ) resulted in excessive deformation, having more molecular water than colemanite mineral [ $Ca_2B_6O_{11} \cdot 5H_2O$ ]. Therefore, it was clearly understood that calcination was a necessary process in order to prevent such the gas transfer which occurs by the decomposition of colemanite mineral in the sintering stage. XRD, SEM, DTA/TG, EDX and light scattering laser diffractometer particle size analysis were applied to the calcined colemanite solid waste (CCSW), proved that calcination was successfully performed on the colemanite solid waste.

Considering the optical dilatometer results and factory conditions, it was decided to apply a sintering temperature of 1130 °C to the R7 porcelain tile bodies in which Na-feldspar was replaced by 5% CCSW (by weight). This sintering temperature was also very close to the temperature, theoretically obtained from the optical

dilatometer. The new sintering temperature of 1130 °C is 80 °C lower than the standard sintering temperature of the factory. Therefore, a small colemanite waste addition to the porcelain tile bodies can provide a considerable amount of energy saving for the factory without changing other operational parameters.

After the physical and mechanical tests applied to the CCSW-added R7 bodies sintered at 1130 °C as well as the XRD and microstructural analysis (SEM-EDX) was carried out, it was seen that the results were almost similar to those of the standard porcelain tile bodies (R1) sintered at 1210 °C. In standard porcelain tile bodies sintered at 1130 °C (R6), however, a homogenous glassy matrix structure did not occur and hence the anorthoclase [ $(Na,K)Si_3AlO_8$ ] phase remained in a non-dissolved state in this glassy phase. This is also an indication that the factory should not change any operational parameter other than decreasing the sintering temperature by 80 °C if Na-feldspar is replaced by 5% CCSW in the standard porcelain tile formulation used. After the XRD, SEM/EDX analyses and physical-mechanical tests applied to the RCSW and CCSW-added bodies it was found that calcination was necessary in order to comply with the required technical specifications in the final product obtained in a fast firing condition.

Finally, it can be said that the use of colemanite waste is advantageous for the porcelain tile industry since it reduces the sintering temperature and raw material cost. The use of the waste may also provide some economic gains in marketing these previously unused wastes.

## Acknowledgements

The authors would like express their gratitude to the administration of Emet Mine of National Boron Board of Turkey for the collection of the wastes and the necessary information; the Management of Kütahya Ceramic Inc. for the provision of production facilities; Prof.Dr. Ferhat KARA (Head of Ceramic Research Centre, Anadolu University) and Prof.Dr. Servet TURAN (Head of Ceramic Engineering Department, Anadolu University) for providing the necessary characterization set-up; Dr. Darron Dixon-Hardy (School of Process, Environmental & Materials Engineering, University of Leeds, UK) for his kind guidance in the paper preparation and Mr. Hilmi YURDAKUL for his invaluable help throughout the research.

## References

1. A.P. Luz and S. Ribeiro, *Ceramics International* 33 (2007) 761-765.
2. R. Gennaro, P. Cappelletti, G. Cerri, M. Gennaro, M. Dondi, G. Guarini, A. Langella and D. Naimo, *Journal of the European Ceramic Society* 23[13] (2003) 2237-2245.
3. W.M. Carty and U. Senapati, *Journal of the European Ceramic Society* 81 (1998) 3-20.

4. E. Sanchez, M.J. Ibanez, J. Garcia-Ten, M.F. Quereda, I.M. Hutchings and Y.M. Xu, *Journal of the European Ceramic Society* 26 (2006) 2533-2540.
5. R. Gennaro, M. Dondi, P. Cappelletti, G. Cerri, M. Gennaro, G. Guarini, A. Langella, L. Parlato and C. Zanelli, *Microporous and Mesoporous Materials* 105 (2007) 273-278.
6. E. Rambaldi, W.M. Carty, A. Tucci and L. Esposito, *Ceramics International* 33 (2007) 727-733.
7. M. Raimondo, C. Zanelli, F. Matteucci, G. Guarini, M. Dondi and J.A. Labrincha, *Ceramics International* 33 (2007) 615-623.
8. H.R. Fernandes and J.M.F. Ferreira, *Journal of the European Ceramic Society* 27 (2007) 4657-4663.
9. S. Ferrari and A.F. Gualtieri, *Applied Clay Science* 32 (2006) 73-81.
10. L. Esposito, A. Salem, A. Tucci, A. Gualtieri and S.H. Jazayeri, *Ceramics International* 31 (2005) 233-240.
11. K. Dana, J. Dey and S.K. Das, *Ceramics International* 31 (2005) 147-152.
12. A. Tucci, L. Esposito, E. Rastelli, C. Palmonari and E. Rambaldi, *Journal of the European Ceramic Society* 24 (2004) 83-92.
13. S. Kurama, A. Kara and H. Kurama, *Journal of the European Ceramic Society* 26, (2006) 755-760.
14. Website of National Boron Board of Turkey (2008) [http://www.etimaden.gov.tr/en/0\\_sayfa\\_ortakSayfa.asp?hangiSayfa=0\\_sayfa\\_Giris](http://www.etimaden.gov.tr/en/0_sayfa_ortakSayfa.asp?hangiSayfa=0_sayfa_Giris). Accessed 2 Feb 2008.
15. B. Karasu, G. Kaya, H. Yurdakul and A. Topkaya, in *Abstract Book of the 104<sup>th</sup> Annual Meeting & Exposition of the American Ceramic Society*, St. Louis, America, 2002, edited by A. Goyal, W. Wang-NG, M. Murakami and J. Driscall p. 274.
16. G. Kaya, B. Karasu and E. Karacaoglu, in *Proceedings of Sohn International Symposium on Advanced Processing of Metals and Materials: Principles, Technologies and Industrial Practice*, San Diego, America, 2006, edited by F. Kongoli and R.G. Reddy p. 535.
17. B. Karasu, G. Kaya and R. Kozulu, in *Abstract Book of the 104<sup>th</sup> Annual Meeting & Exposition of the American Ceramic Society*, St. Louis, America, 2002, edited by A. Goyal, W. Wang-NG, M. Murakami and J. Driscall p. 275.
18. B. Karasu, G. Kaya and R. Kozulu, *Key Engineering Materials* 264-268 (2004) 2505-2508.
19. B. Karasu, G. Kaya and O. Ozdemir, in *Proceedings of Sohn International Symposium on Advanced Processing of Metals and Materials: Principles, Technologies and Industrial Practice*, San Diego, America, 2006, edited by F. Kongoli and R.G. Reddy p. 529.
20. G. Kaya and B. Karasu, in *Proceedings of Austceram & the 3<sup>rd</sup> International Conference on Advanced Materials Processing*, Melbourne, Australia, 2004, edited by J.F. Nie p. 301.
21. B. Karasu, G. Kaya and M. Taykurt, in *Abstract Book of the 9<sup>th</sup> International Ceramic Processing Science Symposium*, Coral Springs, Florida, America, ICPSS-045-2006, p. 25.
22. B. Karasu and G. Kaya, in *Proceedings of Austceram & the 3<sup>rd</sup> International Conference on Advanced Materials Processing*, Melbourne, Australia, 2004, edited by J.F. Nie p. 103.
23. B. Karasu, G. Kaya and M. Taykurt, in *Abstract Book of the 9<sup>th</sup> International Ceramic Processing Science Symposium*, Coral Springs, Florida, America, ICPSS-044-2006, 2006, p. 24.
24. B. Karasu, G. Kaya and M. Karalar, *Key Engineering Materials* 264-268 (2004) 2497-2500.
25. S. Kurama, A. Kara and H. Kurama, *Journal of the European Ceramic Society* 27 (2007) 1715-1720.
26. N. Ediz, H. Yurdakul and A. Ýssi, *Key Engineering Materials* 264-268 (2004) 2457-2460.
27. N. Ediz, A. İssi and H. Yurdakul, *Key Engineering Materials* 264-268: (2004) 2465-2468.
28. S. Targan, A. Olgun, Y. Erdogan and V. Sevinc, *Cement and Concrete Research* 33[8] (2003) 1175-1182.
29. I. Kula, A. Olgun, Y. Erdogan and V. Sevinc, *Cement and Concrete Research* 31[3] (2001) 491-494.
30. Y. Erdoğan, M.S. Zeybek and A. Demirbş, *Cement and Concrete Research* 28[4] (1998) 605-609.
31. S. Targan, A. Olgun, Y. Erdogan and V. Sevinc, *Cement and Concrete Research* 32[10] (2002) 1551-1558.
32. ISO 10545-3, *Ceramic Tile Part-3 (1997) Determination of Water Adsorption, Apparent Porosity, Apparent Relative Density and Bulk Density*, Switzerland.
33. ISO 10545-4, *Ceramic Tile Part-4, Determination of Modulus of Rupture and Breaking Strength*, Switzerland, 1997.
34. O. Yıldız, *Powder Technology* 142[1] (2004) 7-12.
35. W. Smykatz-Kloss, Editor, *Differential Thermal Analysis Minerals and Rocks vol. 11*, (Springer-Verlag, Berlin, 1974), pp. 58-59.
36. I. Waclawska, *Journal of Thermal Analysis* 53 (1998) 519-532.
37. R.E. Grim, in *"Applied Clay Mineralogy"* (Mcgraw-Hill Book Company, New York, Toronto, London, 1962) p. 90.
38. W.R. David, in *"Modern Ceramic Engineering: Properties, Processing, and Use in Design"*, Second Edition, Revised and Expanded" (Marcel Dekker, Inc., 1992) p. 379-381.
39. F. Singer and W.L. German, in *"Ceramic Glazes"* (Borax Consolidated Limited, Borax House, Carlisle Place, London SW1, 1964) p. 1.
40. M. Paganelli, *American Ceramic Society Bulletin* 81[11] (2002) 25-30.
41. J.S. Reed, in *"Principles of Ceramics Processing, Chapter XI"* (New York, 1995) p. 172.
42. F.C. Kracek *Journal of Physical Chemistry*, 36[10] (1932) 2529-2542.
43. E.S. Vilches, in *"Technical Considerations on Porcelain Tile Products and their Manufacturing Process"* (Qualicer, 2002) p. 57.
44. C. Leonelli, F. Bondioli, P. Veronesi, M. Romagnoli, T. Manfredini, G.C. Pellicani and V. Cannillo, *Journal of the European Ceramic Society* 21 (2001) 785-793.
45. L. Carbajal, F. Rubio-Marcos, M.A. Bengochea and J.F. Fernandez, *Journal of the European Ceramic Society* 27 (2007) 4065-4069.
46. R.W. Cahn, P. Haasen and E.J. Kramer, in *"Materials Science and Technology, Vol 11-Structure and Properties of Ceramics"* edited by M. Swain (John Wiley & Sons Inc., 1994) p. 522-523.